The use of grey-taguchi based approach for modeling and Heuristic algorithm-based method for optimization of flux assisted TIG welding Process

Mahdi Mazloom Farsibaf, Masoud Azadi Moghadam, Farhad Kolahan[*]

Department of Mechanical Engineering, Mashhad, Iran, Ferdowsi University of Mashhad, Iran

Abstract

A regression based mathematical modeling and a heuristic based optimization technique in flux assisted TIG known as activated tungsten inert gas (A-TIG) welding process for AISI316L austenitic stainless steel parts is addressed in this paper using Grey-Taguchi approach and simulated annealing (SA) algorithm. Process input parameters considered, were welding current (I), torch speed (S) and welding gap (G). The most important quality characteristics have been taken in to account were depth of penetration (DOP) and weld bead width (WBW). To enhance the welding process performance, an activating flux (TiO2, nano-particle) has been used. To gather the required data for modeling purposes design of experiments (DOE) based on orthogonal array Taguchi (OA-Taguchi) method has been employed. Then, different regression equations have been employed to model the process. Moreover, grey relational analysis (GRA) has been used to model the process outputs as a multi criteria to achieve all considered output simultaneously. The most fitted models were selected based on the statistical analysis performed. Next, simulated annealing (SA) algorithm has been used for optimization of process parameters of the selected models (both single and multi-criteria) in such a way that WBW minimized and DOP and GRG (output of GRA) is maximized. Finally, experimental tests have been carried out to evaluate the performance of the proposed method. Moreover, results of the proposed technique has been compared with ones gained using Taguchi approach (signal to noise (S/N) analysis). Based on confirmation tests, the proposed procedure is quite efficient in modeling and optimization of A-TIG process.

Keywords: activated TIG (A-TIG) welding process; grey relational analysis (GRA); multi criteria optimization; design of experiments (DOE); and simulated annealing (SA) algorithm

1. Introduction

Nowadays, gas tungsten arc welding (GTAW), also known as tungsten inert gas (TIG) welding is one of the most widely used welding processes for fabricating stainless steels parts due to its good quality and surface finish. As TIG welding process produces a shallow penetration, its application for welding of thick parts in a single pass is

---

[*] Corresponding author. Tel.: +989153114112;
E-mail address: kolahan@um.ac.ir

restricted [1, 2].To tackle this problem, different procedures have been introduced. Using activated fluxes coated on the weld surface before welding, known as activated TIG (A-TIG) welding process is one of the important methods used to improve depth of penetration (DOP) and weld bead width (WBW) in TIG welding process of different materials especially for stainless steel parts [3, 4]. This process can be taken in to account as the TIG welding process in which a layer including activating fluxes used on the weld surface before welding process started. These fluxes, are melted and vaporized during the process and due to arc constriction and reversal of Marangoni convection phenomena, DOP and WBW are increased and decreased respectively [5, 6].

A-TIG welding process has been effectively employed on different materials namely: alloy steels, stainless steels including austenite and austenite duplex stainless steels, and dissimilar metals welding [6, 7]. Application of A-TIG welding process, allowed steel parts (of around 6 mm) to be fabricated using a single pass and without even using filler metal [6].

There are different studies in which A-TIG welding process have been studied. In this regard Vidyarthy et al. [8] studied the effect of an activating fluxes on the microstructural, mechanical properties and corrosion behavior of dissimilar welding of AISI316L and P91 steel parts. Effect of an activating flux on DOP, microstructure and mechanical properties of Ti-6Al-4V GTAW welds have been studied by Ramkumar et al. [9]Kulkarni et al. [10]studied the effect of using A-GTAW welding process on mechanical properties in dissimilar welding of Inconel 800 and Inconel 600. Microstructural and mechanical properties of A-GTAW welding process has been studied in refs [5, 6]in fabricating of P91 weldments. Process of GTAW has been optimized using RSM in order to achieve the largest DOP by Pamnani et al. [6] Full penetration has been reported using A-GTAW welding process in comparison with C-GTAW welding process by Kumar et al. [7] Based on the results, A-GTAW welding process could improve the performance of GTAW welding process by increasing DOP and decreasing WBW simultaneously. Elimination of edge preparation before welding process (for specimens with more than 3mm thickness) and reduction of welding passes required for accomplishing fabricating in GTAW welding process has been reported by Venkatesan et al. [11] using activating fluxes. Mechanical properties improvement and reduction of distortion were introduced by Chern et al. [12] as the main assets of A-GTAW welding process. Different fluxes (including oxide, chloride, and fluoride fluxes) have been employed by Tathgir et al. [13] in dissimilar welding process of stainless steel and low alloy parts to improve DOP. Based on the research results, using oxide fluxes results in the largest DOP in comparison with other fluxes. Furthermore, other fluxes had trivial and negligible effect on DOP.

To the best of our knowledge, there is no study in which modeling and optimization of DOP and WBW are considered using design of experiments (OA-Taguchi approach), mathematical modeling (regression modeling), statistical analysis (analysis of variance) and a heuristic algorithm (SA algorithm). Therefore, in this article based on the preliminary experimental tests using design of experiments (screening approach) and literature survey, three inputs parameters (welding current (I), torch speed (S) and welding gap (G)) have been taken into account as adjusting parameters and their corresponding intervals and levels determined. Furthermore, DOP and WBW have been considered as the most important output characteristics. According to the number of input parameters and their levels, the most appropriate design matrix (OA-Taguchi) has been considered. Next, to establish the relations between input parameters and output characteristics on the experimental tests gathered base on the OA-Taguchi design matrix, different regression models (including linear, curvilinear and logarithmic) have been performed. Then, in order to choose the most fitted derived regression equations as the authentic representatives of the process, analysis of variance (ANOVA) has been performed. Furthermore, significance of the process input parameters and their corresponding percent contribution on each output measures have been determined based on the ANOVA results. At the last step, in order to maximize DOP and minimize WBW simultaneously, grey relational analysis (GRA) has been used, to model the A-TIG process output characteristics simultaneously as a single objective. Finally, the optimal values of process input parameters for single and multi-criteria optimization have been determined using simulated annealing (SA) algorithm and signal to noise (S/N) method. The proposed approach has been carried out on AISI316L austenitic stainless steel sheets.

2. Equipment and experimental setup used

To carry out the experiments needed a DIGITIG 250 AC/DC welding machine was used. Furthermore, in this study, Argon (with 99.7% purity) was used as the inert gas.
AISI316L stainless steel sheets with dimension of 100 mm×50 mm×10 mm have been considered as specimens. In this study, titanium dioxide (TiO_2) Nano-powder (+99%, 20-30 nm, amorphous) has been used as the activating flux. The details of preparing and mechanism of A-TIG welding process are well documented in Refs [5, 6].

2.1. Input parameters of A-TIG welding process and their corresponding levels

There are different parameters affecting the A-TIG welding process among which, welding current (I), speed (S) and gap (G) are the most influential ones based on the literature review and screening method used [2, 5, 6]. Similarly, process quality characteristics include DOP and WBW are the most important characteristic of A-TIG welding process. To determine the possible working intervals of each process input parameter, welding references studied and some preliminary tests were conducted [5, 7, 10, 12, 13]. Table 1, lists the process input parameters and their corresponding intervals and levels based on the initial test findings. Other input parameters with trivial effects have been considered at a fixed level.

Table 1 A-TIG welding process input parameters and their levels.

Process parameter	welding gap (G)	Welding current (I)	Torch speed (S)
Unit	mm	Amps	mm/sec
Symbol	G	I	S
Interval	0.75-1.50	100-280	1.00-3.33
Level 1	0.75	100	1.00
Level 2	1.50	160	1.67
Level 3	-	220	2.67
Level 4	-	280	3.33

2.2. Design of experiments (DOE) approach

After selecting the process input parameters and their intervals and levels, an appropriate design matrix to conduct the experiments required to be determined. Generally, to facilitate the identification of the influence of individual parameters, establish the relationships between process input parameters, output characteristics, and finally determine the optimal levels of input parameters in order to get the desired characteristics, DOE approach is used. One of the effective methods that can intensely reduce the number of experiments required to gather necessary data, is OA-Taguchi technique [14]. An OA-Taguchi's L_{32} design matrix has been opted based on the number of input parameters and their corresponding levels (Table 2).

2.3. Experimental results

The accuracy of the procedure, has been increased using a random order in conducting the experiments. After welding, two types of characteristics (DOP and WBW) have been taken from each sample. Fig. 1, displays a specimen welded under the same parameter levels for both C-TIG and A-TIG welding process. As shown, A-TIG process results in smaller WBW and higher DOP.
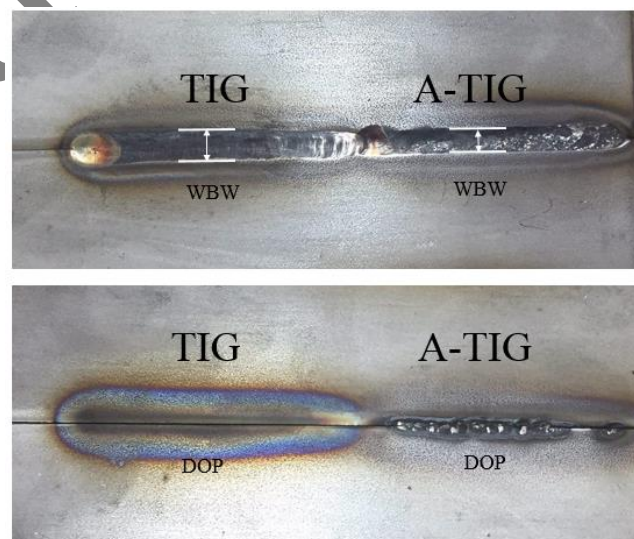
Fig. 1 Comparison of the output characteristics in C-TIG and A-TIG welded samples

For measuring DOP and WBW, on each samples two transverse cross sections were made. Next, to clearly show DOP and WBW, the cut faces were smoothly polished and etched (Fig. 2).

Then, for taking images an optical microscope has been used (Fig. 2). To determine samples' DOP and WBW, images were consequently processed by MIP (microstructural image processing) software (Fig. 4). The average of two measurements for each sample was reported (Table 2).

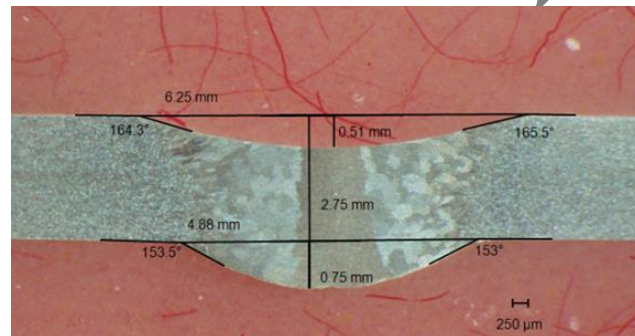**Fig. 2** Optical microscope and electro polish machine used

Fig. 3 Evaluation of DOP and WBW using MIP software

3. Signal to noise ratio

A practical finite element model (FEM) of payload fairing is shown in Fig. 4. The diameter of the payload fairing is 1.5 m. The model is constructed and analyzed in ABAQUS 2020. As shown in Fig. 4, the fairing structure comprises a nose segment, cone segment, and barrel section. When the rocket reaches a certain height, the separation system will begin unlocking.

Finite element modeling and analysis was the primary tool used to design the fairing. Models were developed using available coupon samples and subscale test articles from various manufacturing alternatives and materials. The upper conic and barrel sections were designed assuming an oven-cured, vacuum bagged, sandwich composite, consisting of carbon-fiber/resin T300 face-sheets and honeycomb core made of Nomex and Al-5022. In the structural analysis, the elastic behaviour of Nomex is defined using Liu's [15], and carbon-fiber/resin T300 is defined using Wang's [16] property research.

Table 2. Experimental conditions based on Taguchi approach and their measured outputs and S/N ratios

No	welding gap	Welding current	Torch speed	Penetration (mm)	Weld bead width (mm)	S/N value for DOP	S/N value for WBW	GRG
1	0.75	100	1.00	2.97	4.10	21.7712	-28.2197	0.577780
2	0.75	100	1.67	2.71	4.19	19.9390	-28.6540	0.598948
3	0.75	100	2.67	2.32	3.75	16.8313	-26.4351	0.625378
4	0.75	100	3.33	2.33	3.96	16.7213	-27.0151	0.627714

5	0.75	160	1.00	5.15	6.39	32.7799	-37.0947	0.511789
6	0.75	160	1.67	4.40	5.46	29.6321	-33.9490	0.520790
7	0.75	160	2.67	3.52	5.35	25.1692	-33.5419	0.564611
8	0.75	160	3.33	3.20	5.20	23.2630	-32.9732	0.581755
9	0.75	220	1.00	7.75	7.82	40.9539	-41.1337	0.484357
10	0.75	220	1.67	5.42	7.10	33.8019	-39.2019	0.522525
11	0.75	220	2.67	4.65	7.30	30.7373	-39.7575	0.558822
12	0.75	220	3.33	4.45	6.94	29.8581	-38.7460	0.556181
13	0.75	280	1.00	9.15	9.65	44.2751	-45.3392	0.554476
14	0.75	280	1.67	7.10	9.45	39.2019	-44.9203	0.581329
15	0.75	280	2.67	5.80	9.07	35.1572	-44.0994	0.593843
16	0.75	280	3.33	4.83	9.43	31.4969	-44.8779	0.650982
17	1.50	100	1.00	2.66	4.80	19.8202	-31.1245	0.613655
18	1.50	100	1.67	2.60	4.95	19.1102	-31.9878	0.621403
19	1.50	100	2.67	2.20	4.10	15.7691	-28.2197	0.642242
20	1.50	100	3.33	1.91	4.12	12.9421	-28.3171	0.672495
21	1.50	160	1.00	5.77	6.50	35.0534	-37.4360	0.493209
22	1.50	160	1.67	4.08	7.07	28.1219	-39.1172	0.577849
23	1.50	160	2.67	3.39	5.50	24.4166	-34.0950	0.575752
24	1.50	160	3.33	3.06	5.42	22.3683	-33.8019	0.595871
25	1.50	220	1.00	7.82	8.78	41.1337	-43.4495	0.525907
26	1.50	220	1.67	6.13	9.32	36.2639	-44.6433	0.598763
27	1.50	220	2.67	4.67	7.58	30.8232	-40.5103	0.567667
28	1.50	220	3.33	4.11	7.37	28.2685	-39.9484	0.586134
29	1.50	280	1.00	11.02	10.39	47.9942	-46.8169	0.590101
30	1.50	280	1.67	8.52	11.05	42.8483	-48.0486	0.703986
31	1.50	280	2.67	5.95	9.76	35.6678	-45.5658	0.634413
32	1.50	280	3.33	4.70	9.31	30.9532	-44.2433	0.648665

4. Regression modelling and statistical analysis

Regression modeling is a mathematical approximating in order to determine the relationships between process input parameters and output characteristics. To carry out the regression modeling and statistical analysis procedure, the following stages are to be taken in to account [17, 18]

First, process input parameters and output characteristics are identified. Then, interval for each process input parameter is determined through literature survey, preliminary experiments and screening method. Selection of an appropriate DOE matrix based on the process input parameters and their corresponding levels, such as full factorial design and fractional factorial design is the next step. Next, the experiments are conducted as the matrix opted and data collected. Finally, the process characteristics equations are driven by developing mathematical models and conducting significance test (F-test and P-test) and the most fitted models as the representative of the process characteristics are selected [18].

The process input parameters are shown in Table 2 (2th -4th columns). The next two columns are the measured DOP and WBW based on the conducted experiments in each rows. The last two columns are the calculated S/N ratio values for the measured characteristics. Any of the above output is a function of process parameters which are expressed by linear, logarithmic and second order functions; as stated in Equations 3 to 5 respectively [19].

$$. Y_1 = a_0 + a_1B + a_2C + a_3D \tag{3}$$

$$Y_2 = a_0 + a_1B + a_2C + a_3D + a_{11}BB + a_{22}CC + a_{33}DD + a_{12}BC + a_{13}BD + a_{23}CD \tag{4}$$

$$Y_3 = a_0 \times B^{a1} \times C^{a2} \times D^{a3} \tag{5}$$

Where, regression constants are shown with a_0, a_1, a_2 and a_3 and are to be predicted. Furthermore, B, C and D are the input parameters (I, S, G) and Y_1, Y_2 and Y_3 are the output characteristics (S/N ratio values for DOP and WBW). Based on the calculated S/N ratios for DOPs and WBWs data given in Table 2, the regression equations are developed using MINITAB software.

Models representing the relationship between process input parameters and output characteristics could be stated in Equations 6 to 11.

4.1. Single objective modeling

In this part, the process output characteristics have been modeled using regression modeling. Furthermore, the objective is to optimize each process measure lonely.

4.1.1. Linear Model

$$S/N(DOP)=17.3+1.07\times G + 0.115\times I - 4.90\times S \tag{6}$$

$$S/N(WBW)=-19.4- 2.81\times G - 0.0939 \times I + 1.27 \times S \tag{7}$$

4.1.2. Logarithmic model

$$S/N (DOP) = e^{2.90} \times I^{0.00416} \times S^{-0.163} \tag{8}$$

$$S/N (WBW) = e^{0.00254} \times I^{0.461} \times S^{-0.0320} \tag{9}$$

4.1.3. Second order Model

$$S/N (DOP) = 6.82382 - 5.08171\times S + 0.242879\times I - 0.000329412\times I\times I + 1.12962\times S\times S + 0.0221252\times G\times I - 1.73873\times G\times S - 0.0137971\times I\times S \tag{10}$$

$$S/N (WBW) = -15.4541 - 5.278\times G - 0.127163\times I + 1.25302\times S + 0.000122193\times I\times I + 1.09382\times G\times S - 0.00592234\times I\times S \tag{11}$$

4.2. Multi-criteria modeling

In this part, the DOP and WBW have been modeled simultaneously using grey relational analysis (GRA). Normalizing the raw data (7th and 8th columns of Table 2) is the first step in GRA. Supposing there are n series of data (number of run tests) and in each series m responses (number of dependent variables) measured. Test results are then determined by $y_{i,j}$ (i = 1,2, ..., n and j = 1,2, ..., m).

The following steps are required to perform the GRA [19]:

a) A linear normalization of the experimental values for the responses, namely DOP, and WBW is performed in the range between 0 and 1. In this step, if the higher value of a response is desired, Eq. (12) is used for normalizing which is called "the- highest-the-best" criterion. Thus, DOP is normalized by this equation. When the lower value of a response is preferred, Eq. (13), termed "the-lowest-the-best" criterion, is used for normalizing. By the same token, Eq. (13) is used to normalize observed WBW.

$$Z_{i,j} = \frac{(y_{i,j} - \min(y_{i,j}, i=1,2\ldots,n))}{(\max(y_{i,j}, i=1,2\ldots,n) - \min(y_{i,j}, i=1,2\ldots,n))} \tag{12}$$

$$Z_{i,j} = \frac{(\max(y_{i,j}, i=1,2\ldots,n) - y_{i,j})}{(\max(y_{i,j}, i=1,2\ldots,n) - \min(y_{i,j}, i=1,2\ldots,n))} \tag{13}$$

b) Calculating the grey relational coefficient (GRC) for the normalized values through Eq. (14):

$$\gamma(Z_o, Z_{i,j}) = \frac{\Delta_{min} + \zeta\Delta_{max}}{\Delta_{oj}(k) + \zeta\Delta_{max}} \tag{14}$$

Where: ζ is called the coefficient of distinguishing and its interval is between 0 and 1. The weighting of parameters depends on the relative importance of each response [19]. When weighting coefficients are equal, the value of ζ is set to 0.5. $Z_o(k)$ is called the reference sequence and it could take either the largest or the smallest values given by Eq. (12) and (13). When the higher value of a response is preferred, it is the largest value among all $Z_{i,j}$; and when the lower value of a response is desired, $Z_o(k)$ takes the smallest value of all $Z_{i,j}$. Δ_{oj} is the absolute value of the difference between $Z_o(k)$ and $Z_{i,j}(k)$; $\Delta_{oj} = |Z_o(k) - Z_{i,j}|$. Δ_{min} and Δ_{max} are the smallest and the largest value of difference between $Z_o(k)$ and $Z_{i,j}(k)$ which are given by:

$$\Delta_{min} = \min|Z_o(k) - Z_{i,j}| \quad \Delta_{max} = \max|Z_o(k) - Z_{i,j}| \tag{15}$$

c) Computing grey relational grade (GRG) for any response using Eq. (16):

$$\text{Grade}(Z_o, Z_{i,j}) = \sum_{k=1}^{n} \beta_k \gamma(Z_o, Z_{i,j}) \tag{16}$$

Where:

$$\sum_{k=1}^{n} \beta_k \gamma(Z_o, Z_{i,j}) = 1 \tag{17}$$

In the above, β_k is the weighting factor of each response [19]. Results of *GRGs* have been presented on the last column of Table 2. Eq. (18), represents the multi-criteria model of the process considering DOP and WBW simultaneously.

S/N (Multi) = 0.775633 + 0.0575675×G - 0.00355061×I + 0.0297328×S - 0.00968507×G×S + 8.83284e-006×I×I

+ 4.35804e-005×I×S   (18)

4.3. Performing analysis of variance (ANOVA)

To determine the adequacy of the proposed models, how well a model fits the experimental data and represents the authentic process under study, analysis of variance (ANOVA) is performed [21]. ANOVA procedure within 95% of confidence limit has been employed to check the adequacies of proposed regression models (Table 3) [19]. Obviously, the second order/modified second order model (with elimination of unimportant parameters) for DOP and GRG and logarithmic model for WBW are the superior models to other models based on the required confidence limit (Pr), the correlation factor (R^2) and the adjusted correlation factor (R^2-adj). Thus, these superior models are considered as the best authentic representative of the A-TIG welding process in this paper.

Table 3. ANOVA results of different models for the A-TIG welding process charactristics

	Model	Variable	R^2	R^2 (adj)	F-value	Pr>F
Single Objective Models	Linear	DOP	95.7%	95.2%	185.90	<0.0001
	logarithmic	DOP	92.2%	91.6%	152.83	<0.0001
	Second order	DOP	99.4%	99.2%	489.21	<0.0001
	Linear	WBW	95.7%	95.4%	258.86	<0.0001
	logarithmic	WBW	92.6%	92.0%	161.88	<0.0001
	Second order	WBW	98.1%	97.8%	271.16	<0.0001
Multi Objective Models	Linear	GRG	75.23%	74.64%	189.95	<0.0001
	logarithmic	GRG	85.32%	83.47%	215.82	<0.0001
	Second order	GRG	96.01%	94.93%	521.95	<0.0001

Figs 4, 5 and 6 illustrate the residual plots (including normal portability, residual versus fitted values, histogram, and residual versus observation order) for DOP, WBW and GRG respectively in which a good conformability of the developed models to the real process have been demonstrated. The details about the performing of ANOVA has been well documented in ref [19].

Tables 4, 5 and 6 show the detailed results of ANOVA for S/Ns values of DOP and WBW and GRG. Large F–value illustrates that the variation of the process parameter makes a big change on the performance of the process. In this study, to evaluate parameters significances a 95% confidence level is selected. Therefore, F–values of A-TIG process parameters are compared with the appropriate values from confidence table, $F_{\alpha,v1,v2}$; where α is risk, degrees of freedom associated with numerator and denominator illustrated in Tables 4, 5 and 6 are shown by v_1 and v_2 [19]. Within a confidence limit of 95%, ANOVA results show that welding current, torch speed and welding gap are respectively the most important input parameters affecting DOP and WBW.
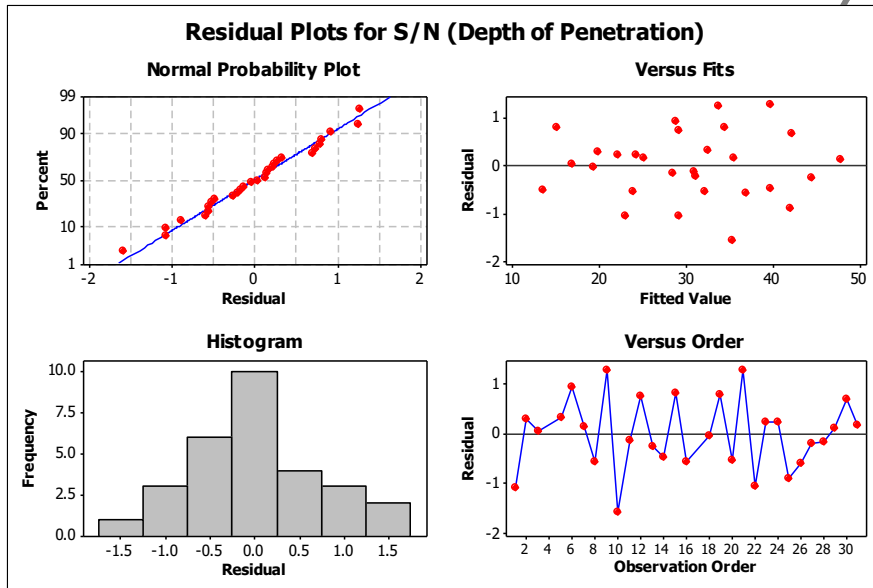

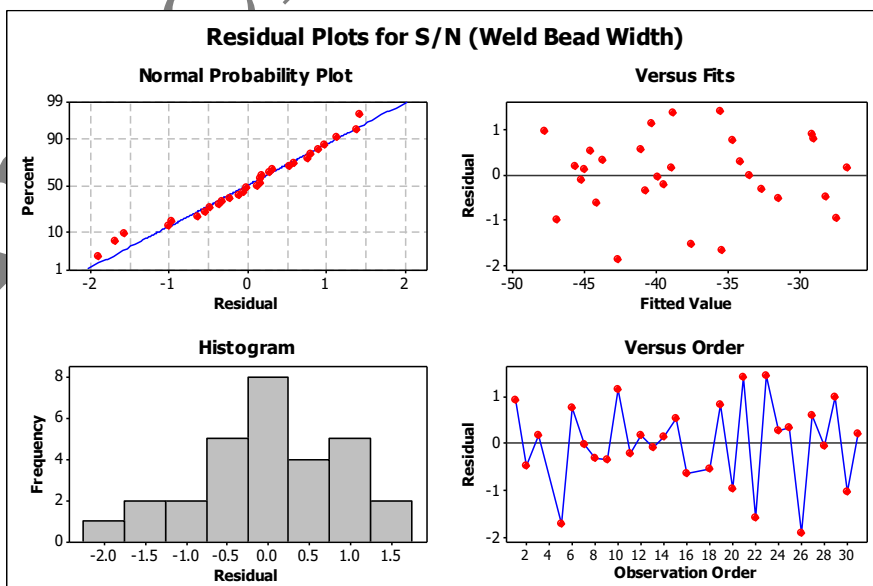**Fig 4**. Residual plot for depth of penetration (DOP)

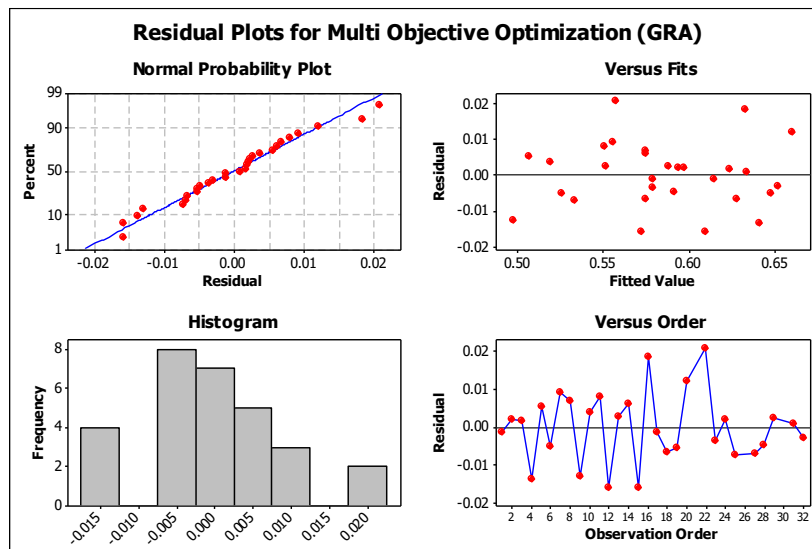**Fig 5.** Residual plot for weld bead width (WBW)

Fig 6. Residual plot for grey relational grade (GRG)

The percent contributions of each parameter may be provided by ANOVA results (Eq. 19) [19]. The percent contributions of the A-TIG process parameters are shown in Figs. 7, 8 and 9.

$$P_i\,(\%) = \frac{SS_i - (DOF_i \times MS_{error})}{Total\ Sum\ of\ Squre} \tag{19}$$

Where, percentage of contribution for each parameters under consideration has been shown by P_i, SS_i is sum of square, DOF_i is degree of freedom of ith factor, and MS_{error} is mean sum of square of error [19].
According to Table 4, welding current is the major factor affecting DOP with 67% contribution. It is followed by torch speed and welding gap with 27% and 1% respectively. The rest (1%) is due to error and uncontrollable parameters based on the nature of the process and the equipment used is acceptable. By the same token, welding current with 90% contribution is the most important parameter affecting WBW. Significant parameters affecting GRG shown in Table 6.

Table 4. Result of ANOVA for S/N of Depth of Penetration						
parameters	DOF	Sum of square (SS$_j$)	Mean Square	F-Value	P-Value	Percent contribution (%)
Regression	7	2274.61	324.944	489.210*	0.0000000	-
S	1	633.21	8.074	12.155*	0.0022016	27
I	1	1552.55	107.719	162.174*	0.0000000	67
I*I	1	47.02	38.952	58.643*	0.0000002	2
S*S	1	10.14	10.832	16.308*	0.0005929	1
G*I	1	7.45	19.051	28.681*	0.0000260	1
G*S	1	9.96	14.511	21.847*	0.0001298	1
I*S	1	14.28	14.283	12.504*	0.0001417	0
Error	21	13.95	-	-	-	1
Total	28	2288.56	-	-	-	100
Significant Parameter *						

parameters	DOF	Sum of square (SS_j)	Mean Square	F-Value	P-Value	Percent contribution (%)
Regression	6	1137.46	189.577	183.956*	0.000000	-
G	1	15.19	15.363	14.908*	0.000846	1
I	1	1074.03	33.172	32.188*	0.000010	90
S	1	34.73	1.457	1.413	0.047157	1
I*I	1	6.68	5.471	5.308*	0.031046	1
G*S	1	4.17	3.408	3.307*	0.042642	1
I*S	1	2.66	2.585	0.022135	0.022135	2
Error	22	22.67	-	-		4
Total	28	1160.13	-	-	-	100
Significant Parameter *						

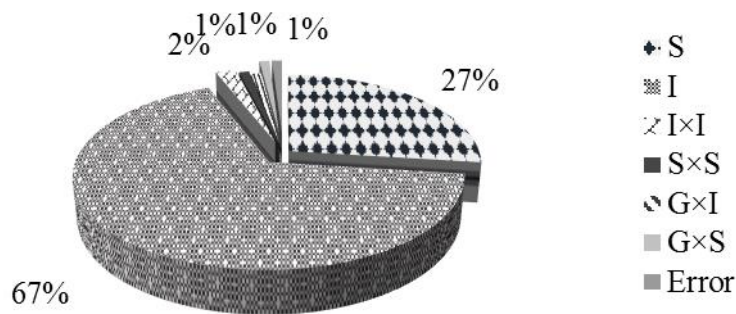**Table 5.** Result of ANOVA for S/N of Weld Bead Width

Fig. 7 Percent contributions of machining parameters to the DOP
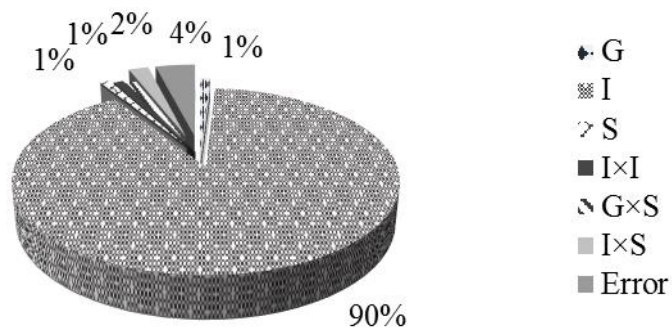

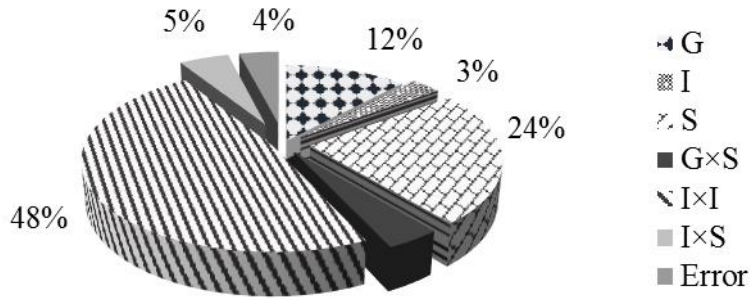**Fig. 8** Percent contributions of machining parameters to the WBW

Fig. 9 Percent contributions of machining parameters to the GRG

5. Optimization procedure

5.1. Taguchi based optimization method

   To define the effect of each process input parameters on the output characteristics, the mean of *S/N* ratios for each test containing this parameter in desired level are calculated. Moreover, the calculated means for each level of input parameter under consideration are compared and the level to which the highest value is belongs considered as the desired level in order to optimize the process characteristic [19]. For example mean effect of torch speed in level 1 is gained from averaging test runs number 1, 2 up to 16. Along these lines, the mean effects of parameters are computed and listed in Tables 7, 8 and 9. Since the higher value of mean *S/N* is favorable, with respect to the data in Table 7, optimal set of parameters for optimization of DOP are: *G* at level 1, *I* at level 4 and *S* at level 1, i.e., (G_1 I_4 S_1). Similarly, optimal set of parameters for optimization of WBW are: *G* at level 1, *I* at level 1 and *S* at level 3, i.e., ($G_1 I_1$ S_3) based on results of Table 8. Likewise, optimal set of parameters for optimization of GRG are: *G* at level 2, *I* at level 1 and *S* at level 4, i.e., ($G_2 I_1$ S_4) based on results of Table 9.

Table 7. Response (mean) of S/Ns for depth of penetration

Symbol	Level 1	Level 2	Level 3	Level 4
G	**29.47433**	29.47216	-	-
I	17.86305	27.60055	33.98006	**38.44933**
S	**35.4727**	31.1149	26.82146	24.48393

Table 8. Response (mean) of S/Ns for weld bead width

Symbol	Level 1	Level 2	Level 3	Level 4
G	**-36.6224**	-38.5828	-	-
I	**-28.7466**	-35.2511	-40.9238	-45.4889
S	-38.8268	-38.8153	**-36.2404**	-36.5281

Table 9. Response (mean) of S/Ns for GRG

Symbol	Level 1	Level 2	Level 3	Level 4
G	0.5695	**0.6030**	-	-
I	**0.6225**	0.5527	0.5500	0.6197
S	0.5439	0.5907	0.5953	**0.6150**

   As the S/N method in optimization procedure could only determine the best set of process input parameters levels from the pre-determined ones on the design matrix used (Table 2). Using heuristic algorithms (e.g. simulated

annealing, genetic, tabu search and particle swarm optimization) would help interpolating the answer space in order to find the best solution which may not be in the design matrix. In this study the most fitted models selected, consider as the objective functions for the heuristic algorithm used. Therefore, in order to optimize the objective functions simulated annealing (SA) algorithm has been used.

5.2. Simulated annealing algorithm

To tackle the problem of interpolating between the process input parameters levels in order to select the best input parameters values to reach the desired output characteristics, using Taguchi approach or other DOE methods, heuristic algorithms (including SA) are introduced. All heuristic algorithms are reminiscent of biological or physical processes. In this regard, SA is reminiscent of annealing process in heat treatment [20]. In annealing process, heated metals are slowly cooled down to make them reach a state of low energy. First, metals are heated up to a specific and pre-determined temperature, which is above the melting point. Therefore, at this temperature, all particles of the metal are in intense random motion. Then, the metal is slowly cooled down. All particles rearrange themselves and tend to be toward a low energy state. As the cooling process is conducted appropriately slowly, lower and lower energy states are gained until the lowest energy state is reached. At the same token, in A-TIG welding process an energy function is created and minimized. The lowest energy level gives the optimized value of A-TIG welding process parameters, while minimizing efforts are made to avoid local minima and to achieve global minima. Recently, the SA algorithm has developed as a leading tool for complex optimization problems [20, 21]. The mechanism of SA algorithm is defined as follows.

Generating an initial random solution in an acceptable answer space. Then, the objective function of new solution (C_1) is calculated and compared with that of current solution (C_0). A move is made to the new solution, either the new solution has better value or the probability function implemented in SA (Eq. (20)) has a higher value than a randomly generated number between 0 and 1 [20].

$$P_r = \exp\left(-\frac{\Delta c}{\tau_k}\right) \tag{20}$$

Where, temperature parameter is shown by T_k, it plays a similar role as the temperature in the physical annealing process [25]. Eq (21), is used as a temperature reduction rate to cool down the pre-determined temperature at each steps.

$$T_{k+1} = \alpha \times T_k \qquad k = 0,1,... \quad \text{and} \quad 0.9 \leq \alpha < 1 \tag{21}$$

Where, the current and former temperatures are shown by T_{k+1} and T_k respectively. The cooling rate also presented by parameter α. Consequently, at the first iterations of SA, most worsening moves may be accepted due to higher temperature, but at the end, only improving ones are likely to be allowed. This can help the process avoid being trapped in local minimum and jump out of it. After a specific number of iterations or after a pre-determined run time or after a number of iterations in which no development is detected, the algorithm may be terminated.

The results of single and multi-criteria optimization using Taguchi and SA algorithm has been shown in Table 10. As illustrated in Table 10, for resulting in maximum possible DOP, the welding current and welding gap should be considered at their highest levels. Likewise, for achieving lower WBW, welding current and welding gap should be approximately set at their lower ranges.

The SA algorithm convergence for DOP is shown in Fig. 10.

Table 10. Results of optimization based on the Taguchi and SA algorithm

parameters	Set of Parameters				Predicted S/N value	Experimental S/N value	Error (%)	Improvement value
	output	G	I	S				
Best set of parameters in L_{32} experiments	Setting Levels for optimized DOP	1.50	280	1.00	46.0517	-	-	-
	Setting Level for optimized WBW	0.75	100	1.67	-26.9094	-	-	-
Taguchi optimization	Setting Levels for	1.50	280	1.00	46.0517	-	-	-

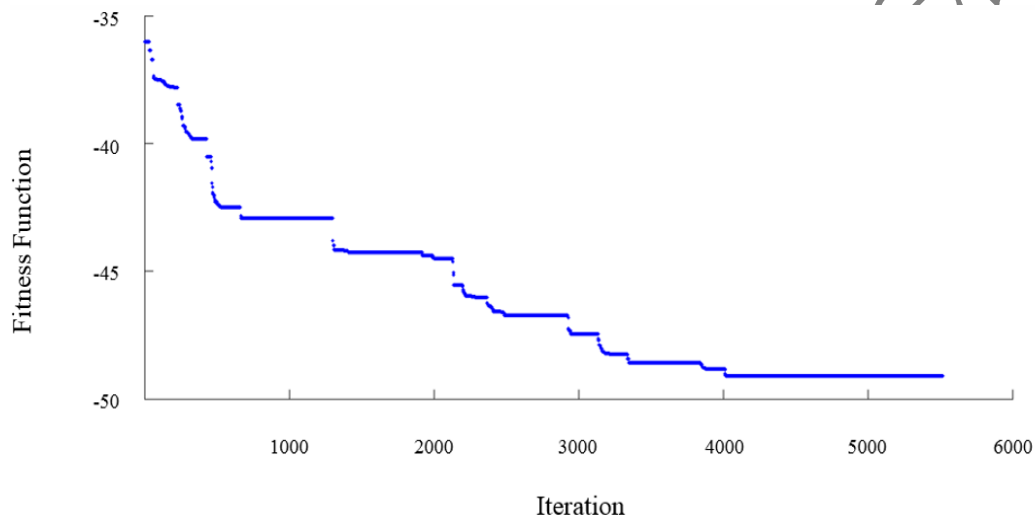|							
	optimized DOP							
	Setting Level for optimized WBW	0.75	100	3.33	-27.0133	-	-	-
Simulated annealing algorithm optimization	Setting Levels for optimized DOP	1.50	280	1.04	49.6648	48.2256	2.9	2.1739
	Setting Level for optimized WBW	1.00	153	2.85	-21.7038	-20.9952	3.3	5.9138
Multi Objective Optimization	Setting Level for optimized GRG	1.00	280	1.00	0.8935	0.8598	3.7	0.1559

Fig. 10 Simulated annealing algorithm convergence for DOP optimization

6. Conclusion

The quality of weldments in A-TIG welding process has been affected by proper selection of process parameters levels. The problem of modeling and optimization of A-TIG welding process for AISI316L austenite stainless steel has been addressed throughout this study. First, A-TIG welding modeling has been performed based on experimental data gathered as per L_{32} OA-Taguchi DOE approach. Then, DOPs and WBWs have been measured using MIP software. Then, S/N approach has been used to formulate the DOP and WBW values. Furthermore, for multi criteria modeling, GRA method has been employed. Next, regression modeling has been used to establish a relation between process characteristics (S/N of DOP, WBW and GRG) as a function of input parameters (welding current, torch speed and welding gap). Next, ANOVA has been used in order to evaluate the adequacy of the proposed models and determine the most fitted ones. Moreover, important parameters and their corresponding percent contribution on each process characteristics has been determined using statistical analysis. Results showed that welding current is the most important parameter affects DOP and WBW with 67% and 90% percent contribution respectively. Furthermore, the minor effect belongs to welding gap. Next, SA algorithm and Taguchi optimization procedure (signal to noise analysis) have been used to optimize the selected models and results confirmed using experimental tests. Furthermore, GRA method has been used for multi-criteria modeling considering both WBW and DOP simultaneously. The result of optimization procedure shows the proposed method can accurately simulate and optimize the A-TIG welding process.

References

[1]   V. M. Sivakumar J, Korra, N . , Effect of activated flux tungsten inert gas (A-TIG) welding on the mechanical properties and the metallurgical and corrosion assessment of Inconel 625, *Welding in the World,* Vol. 65, No. 5, pp. 1065-1077, (2021).

[2]   A. M. Neelima P, Saravanan K, Chakravarthy P, Narayana Murty SVS, Sivakumar Pant D Optimisation of Flux and Weld Parameters During Flux Bounded Tungsten Inert Gas Welding (FBTIG) of Nickel Based Superalloy Inconel 600. , *Transactions of the Indian National Academy of Engineering, : ,* Vol. 6, No. 1, pp. 123-131, (2021).

[3]   K. N. Sivakumar J, N Optimization of Welding Process Parameters for Activated Tungsten Inert Welding of Inconel 625 Using the Technique for Order Preference by Similarity to Ideal Solution Methodology, *Arabian Journal for Science and Engineering,* Vol. 46, No. 5, pp. 7409-7418, (2021)

[4]   B. S. Dhananjay S, Shrikant F, Thorat B Effect of Different Activated Fluxes on Mechanical Properties of DSS 2205 in Pulsed Tungsten Inert Gas Welding. , *Advances in Additive Manufacturing and Joining. ,* Vol. 54, No. 8, pp. 619-629, (2021)

[5]   D. D. Vidyarthy R S, Microstructural and mechanical properties assessment of the P91 A-TIG weld joints, *Journal of Manufacturing Processes. ,* Vol. 31, No. 5, pp. 523-535, (2018)

[6]   B. V. Dhandha KH, Effect of activating fluxes on weld bead morphologyof P91 steel bead-on-plate welds by flux assisted tungsten inert gas welding process. , *Mater Manuf Processes* Vol. 17, No. 2, pp. 48-57, (2105)

[7]   B. A. Tathgir S, Activated-TIG welding of different steels: influence of various flux and shielding gas, *Mater Manuf Process,* Vol. 31, No. 5, pp. 335-342, (2015)

[8]   K. A. Vidyarthy R S, Dwivedi D K Study of microstructure and mechanical property relationships of A-TIG welded P91-316L dissimilar steel joint. , *Materials Science and Engineering A. ,* Vol. 695, No. 45, pp. 249-257, (2017)

[9]   V. V. Ramkumar K D, Prasad M, Rajan N D Effect of activated flux on penetration depth, microstructure and mechanical properties of Ti-6Al-4V TIG welds, *Journal of Materials Processing Technology,* Vol. 261, No. 42, pp. 233-241., (2018)

[10]   V. M. Kulkarni A, Dwivedi DK, Dissimilar metal welding of P91 steel-AISI 316L SS with Inconel 800 and Inconel 600 interlayers by using activated TIG welding process and its effect on the microstructure and mechanical properties, *Journal of Materials Processing Technology,* Vol. 274, No. 5, pp. 116-128., (2019)

[11]   H. C.-Y. Tseng K-H, Performance of activated TIG process in austenitic stainless steel welds., *J Mater Process Technol* Vol. 211, pp. 503-12, (2011)

[12]   T. K-H, Development and application of oxide-based flux powder for tungsten inert gas welding of austenitic stainless steels. , *Powder Technol,* Vol. 233, No. 5, pp. 72-9, (2103)

[13]   T. K. H. Chern T S, Tsai HL Study of the characteristics of duplex stainless steel activated tungsten inert gas welds, *Materials and Design,* Vol. 32, No. 5, pp. 255-263, (2011)

[14]   K. F. Azadi Moghaddam M, Application of orthogonal array technique and particle swarm optimization approach in surface roughness modification when face milling AISI1045 steel parts., *J Ind Eng Int* Vol. 12, No. 2, pp. 199–209, (2016).

[15]   L. Liu, P. Meng, H. Wang, Z. Guan, The flatwise compressive properties of Nomex honeycomb core with debonding imperfections in the double cell wall, *Composites Part B: Engineering,* Vol. 76, pp. 122-132, 2015.

[16]   W. Wang, Y. Dai, C. Zhang, X. Gao, M. Zhao, Micromechanical modeling of fiber-reinforced composites with statistically equivalent random fiber distribution, *Materials,* Vol. 9, No. 8, pp. 624, 2016.

[17]   D. Vishnu, Asal, RI, Patel, T, Alok, B Optimization of Process Parameters of EDM Using ANOVA Method, *International Journal of Engineering Research and Applications,* Vol. 3, pp. 1119-1125, (2013)

[18]   P. V. Vishwakarma M, Regression Analysis and Optimization of Material Removal Rate on Electric Discharge Machine for EN-19 Alloy Steel, *International Journal of Scientific and Research Publications* Vol. 2, No. 2, pp. 167-175, (2102)

[19]   A. M. M. Kolahan F, The use of Taguchi method with grey relational analysis to optimize the EDM process parameters with multiple quality characteristics, *Scientia Iranica* Vol. 22, pp. 530-538, (2015).

[20]   T.-M. R. Jahromi MHMA, Makui A, Shamsi A Solving an one-dimensional cutting stock problem by simulated annealing and tabu search, *Journal of Industrial Engineering International . ,* Vol. 8, No. 2, pp. 1-8, (2012)

[21]   G. C. Kirkpatrick S, Vecchi MP Optimization by simulated annealing, *American Association for the Advancement of Science* Vol. 220, No. 2, pp. 671–680, (1983)